Bioorganic & Medicinal Chemistry 21 (2013) 5963–5972

Contents lists available at ScienceDirect

Bioorganic & Medicinal Chemistry

journal homepage: www.elsevier.com/locate/bmc

Discovery of a novel 5-carbonyl-1*H*-imidazole-4-carboxamide class of inhibitors of the HIV-1 integrase–LEDGF/p75 interaction ☆

Erik Serrao [a,†,‡], Zhong-Liang Xu [b,†], Bikash Debnath [a,§], Frauke Christ [c], Zeger Debyser [c], Ya-Qiu Long [b,*], Nouri Neamati [a,*,§]

[a] Department of Pharmacology and Pharmaceutical Sciences, School of Pharmacy, University of Southern California, Los Angeles, CA 90089, USA
[b] CAS Key Laboratory of Receptor Research, Shanghai Institute of Materia Medica, Chinese Academy of Sciences, 555 Zuchongzhi Road, Shanghai 201203, China
[c] Laboratory for Molecular Virology and Gene Therapy, Division of Molecular Medicine, Katholieke Universiteit Leuven (KULeuven), Kapucijnenvoer 33, B-3000 Leuven, Flanders, Belgium

ARTICLE INFO

Article history:
Received 21 April 2013
Revised 17 July 2013
Accepted 26 July 2013
Available online 2 August 2013

Keywords:
HIV-1
Integrase
LEDGF/p75
5-carbonyl-1H-Imidazole-4-carboxamide
Protein–protein interaction
Antiviral
PDB ID code2B4J

ABSTRACT

Though much progress has been made in the inhibition of HIV-1 integrase catalysis, clinical resistance mutations have limited the promise of long-term drug prescription. Consequently, allosteric inhibition of integrase activity has emerged as a promising approach to antiretroviral discovery and development. Specifically, inhibitors of the interaction between HIV-1 integrase and cellular cofactor LEDGF/p75 have been validated to diminish proviral integration in cells and deliver a potent reduction in viral replicative capacity. Here, we have contributed to the development of novel allosteric integrase inhibitors with a high-throughput AlphaScreen-based random screening approach, with which we have identified novel 5-carbonyl-1*H*-imidazole-4-carboxamides capable of inhibiting the HIV-1 integrase–LEDGF/p75 interaction in vitro. Following a structure–activity relationship analysis of the initial 1*H*-imidazole-4,5-dicarbonyl core, we optimized the compound's structure through an industrial database search, and we went further to synthesize a selective and non-cytotoxic panel of inhibitors with enhanced potency.

1. Introduction

Traditionally, HIV-1 drug development research has focused on inhibiting the active sites of viral enzymes.[1–3] The first HIV-1 integrase (IN) inhibitor (raltegravir) approved by the FDA in October of 2007 was believed to function by chelating the metal cofactor in the active site.[4] Though raltegravir was shown to inhibit viral replication in the low nanomolar range and exhibit a relatively low degree of cellular toxicity,[5] an assortment of viral resistance mutations have limited the plausibility of its long-term prescription.[6] A significant effort has been assigned to the generation of me-too analogues of raltegravir in recent years in the hopes of circumventing viral resistance, but escape mutants have steadily developed in the clinic.[7–9] Indeed, all currently prescribed active site-directed HIV-1 inhibitors have led to the generation of potency-limiting resistance.[10] Combination of potent antiretrovirals into drug cocktails has transformed the management of treatment-experienced patients by delivering a durable knockdown of viral load, viral transmission, and chronic host immune activation,[11–13] but viral eradication looks to require novel modes of enzymatic inactivation.

Allosteric inhibition of IN catalytic activity has emerged as an interesting trend in current antiretroviral drug design and discovery.[14] The rationale is that targeting a non-active-site region on IN that is still essential for its catalysis, such as a cofactor binding site or dimerization hotspot, could yield the same inhibitory potency as active site inhibitors, yet evoke a divergent panel of viable resistance mutations. Hence, addition of an allosteric IN inhibitor

Abbreviations: IN, HIV-1 integrase; LEDGF/p75, lens epithelium-derived growth factor/p75; HBD, hydrogen bond donor; HBA, hydrogen bond acceptor; IC_{50}, 50% inhibitory concentration; EC_{50}, 50% effective concentration; CC_{50}, 50% cytotoxic concentration; $CCID_{50}$, cell culture infective dose.

* Corresponding authors. Address: University of Michigan College of Pharmacy, North Campus Research Complex, 2800 Plymouth Road, Bldg 520, Room 1364, Ann Arbor, MI 48109-2800, USA. Tel.: +1 323 442 2341; fax: +1 323 442 1390 (N.N.).
E-mail addresses: yqlong@mail.shcnc.ac.cn (Y.-Q. Long), Neamati@umich.edu (N. Neamati).
† These authors equally contributed to this work.
‡ Address: Department of Cancer Immunology and AIDS, Dana-Farber Cancer Institute, Harvard Medical School, Boston, MA 02215, USA.
§ Address: Department of Medicinal Chemistry, College of Pharmacy, North Campus Research Complex, University of Michigan, Ann Arbor, MI 48109, USA.

0968-0896/$ - see front matter © 2013 The Authors. Published by Elsevier Ltd. All rights reserved.
http://dx.doi.org/10.1016/j.bmc.2013.07.047

to antiretroviral therapy regimens should deliver a sharp initial reduction in viral copies/mL. By far the most studied cellular cofactor of HIV-1 integration to date is lens epithelium-derived growth factor/p75 (LEDGF/p75). This human protein was originally found to colocalize with IN and stimulate its activity[15] and later found to exert this stimulation by tethering IN to host cell chromatin.[16] In a proof-of-concept study that validated the LEDGF/p75–IN interaction as an antiviral target, the IN-binding LEDGF/p75 domain was overexpressed in human cells and was proven to compete for IN binding with the endogenous full-length cofactor, thereby inhibiting HIV replication.[17]

Since these initial discoveries, the IN-LEDGF/p75 interface has been identified,[18,19] and an initial panel of small-molecules has been rationally developed to bind to this interface and potently inhibit the IN–LEDGF/p75 interaction.[20–22] These molecules are on their way to clinical development, but a diversity of structural classes of IN-LEDGF/p75 inhibitors is essential for the advancement of the field. Here, we have contributed to this field with the identification of a novel class of 5-carbonyl-1*H*-imidazole-4-carboxamide inhibitors of the IN–LEDGF/p75 interaction, which have achieved in vitro inhibition of the IN–LEDGF/p75 interaction in the nanomolar range. Rational synthesis of optimized analogues increased the potency of our inhibitors, and all compounds developed herein were non-cytotoxic in MT-4 cells.

2. Chemistry

Based on the hit (compound **1**) that was identified by high-throughput screening, SAR study and pharmacophore exploration were conducted with respect to the optimal substituents at the 4,5-dicarboxyl sites. As outlined in Scheme 1, a series of 5-carbonyl-1*H*-imidazole-4-carboxamides (**2**–**16**) were designed and synthesized by incorporating different aromatic rings into position 4 and different aliphatic amino moieties into position 5.

The 5-formyl-1*H*-imidazole-4-carboxamide analogues were synthesized according to the literature-reported methodology[23,24] with our modification. As depicted in Scheme 2, the imidazole-4,5-dicarboxylic acid was readily converted to the 1*H*-imidazole-4,5-dicarbonyl dichloride in 89% yield by treating with $SOCl_2$ in toluene with catalytic DMF, followed by esterification with phenol to afford the key intermediate **17** in 94% yield. Nucleophilic addition–elimination of the lactam dimer **17** by various amines produced amide-ester **18a**–**c**. On one hand direct saponification of **17** immediately after aminolysis yielded the acid-amides **2**, **3**, **5**, **6** and **7** in good isolated yields (55–72% for two steps). On the other hand, the nucleophilic attack of the ester-amide **18a** or **18b** by hydrazine or various amines under heating or microwave irradiation generated the asymmetric 4,5-dicarboxamide **8**–**10**, and **14**–**16** in an overall yield of 62–87%, Further treatment with 20% $Pd(OH)_2/C$ to remove the benzyl protection group afforded **18c**-derived compounds **11**–**13**. For the synthesis of 4-hydroxypiperidinyl carboxamide containing compounds (**9**, **12**), an additional saponification was required to remove the acetate protecting group on the 4-hydroxy group.

3. Results

3.1. High-throughput screening generated a hit 4-(phenylcarbamoyl)-1*H*-imidazole-5-carboxylic acid compound

Toward the discovery of novel inhibitors of the IN–LEDGF/p75 interaction, we initiated a high-throughput screening effort using our in-house library of over 50,000 unique compounds. To acquire this library, we previously built a drug-like model considering approximately, 3200 FDA-approved small-molecules and drugs in clinical trials,[25,26] as well as approximately, 11,000 toxic and carcinogenic compounds,[27–30] using machine learning technique (Decision forest) within Pipeline Pilot (Accelyrs, Inc.). The whole dataset was divided into training and test sets randomly consisting of both good (drug) and bad (non-drug) molecules. The training set was used to generate the model, and the test set was used for the purpose of validation of this model. A decision forest of 25 decision trees was used to generate the drug-like model, where decision trees were built using a recursive portioning method. In the test set, out of 1638 drugs, 1335 drugs are predicted as drugs and out of 5666 toxic compounds, 5031 are predicted as toxics, which proves the robustness of the model. We have used the drug-like model to filter eight million commercially available compounds from Asinex, Enamine, Vitas M Laboratory, etc.,[31–33] which resulted in an approximate output of five million drug-like structures. We went further to cluster these compounds using 2D fingerprinting (EFCP-6) and the Tanimoto coefficient to derive a final in-house library of 50,000 diverse compounds representing the chemical space of 8 million. We have procured these compounds in 1 mg scale from these commercial vendors and have demonstrated the utility of this library in generating unique and potent inhibitors of HIV-1 IN catalysis.[34–36]

Using an AlphaScreen® assay previously validated for sensitive and specific detection of inhibition of the IN–LEDGF/p75 interaction,[20,22] we randomly screened 10,000 unique compounds from our in-house library. Of multiple chemical classes of inhibitors identified, we selected 4-(phenylcarbamoyl)-1*H*-imidazole-5-carboxylic acid (compound **1**, Fig. 1) for further development, based on the simplicity of its structure and potency in vitro (IC_{50} = 6 ± 4 - μM). This particular compound was non-cytotoxic in MTT assay and exhibited specificity for inhibition of IN-LEDGF/p75, as it was inactive in our quench counter-screen assay (Table 1). We have previously described the details of this assay.[37] Interestingly, compound **1** was ineffective at inhibiting IN enzymatic activity in terms of 3′-processing and strand transfer (Table 1), differing from what has been recently observed with separate classes of IN-LEDGF/p75 inhibitors.[38]

Compound **1** was docked into the LEDGF/p75 binding site of HIV-1 IN (PDB: 2B4J) for exploration of predicted binding mode,

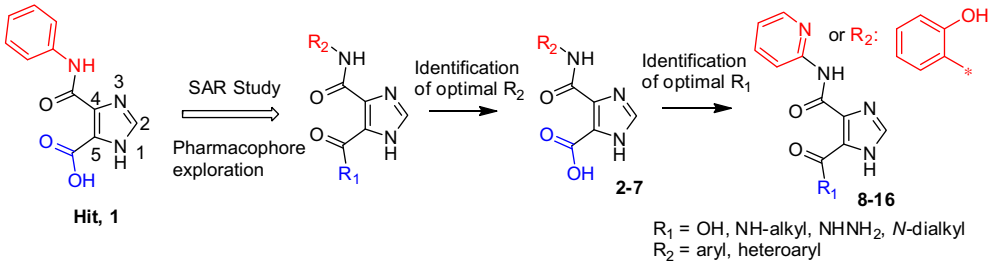

Scheme 1. The medicinal chemistry approach for the SAR study and structural optimization based on the HTS hit and molecular docking.

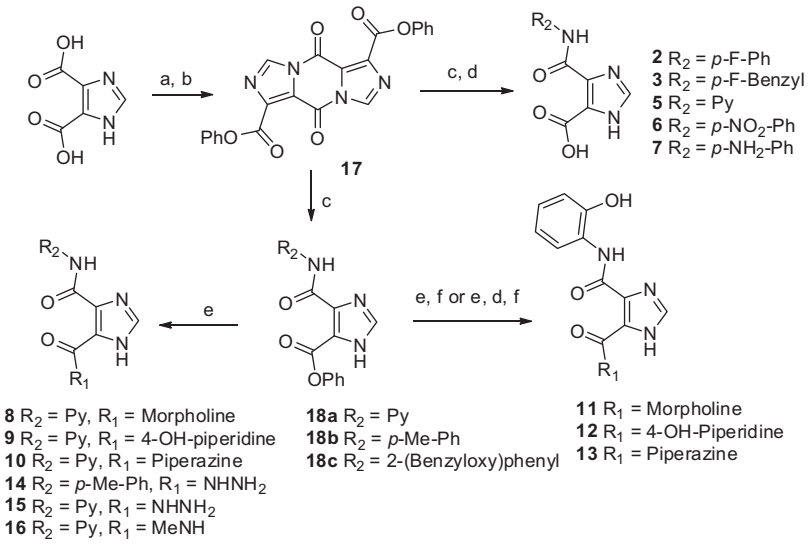

Scheme 2. Reagents and conditions: (a) $SOCl_2$, toluene, cat. DMF, 50 °C; (b) phenol, pyridine (Py), DCM, 0 °C to rt; (c) R_2NH_2, THF; (d) LiOH, THF/H_2O, rt; (e) R_1NH_2, THF, 50 °C or R_1NH_2, DMF, MW, 130 °C (for the heterocyclic amide containing compounds **8**–**13**); (f) 20% $Pd(OH)_2$/C, MeOH, rt.

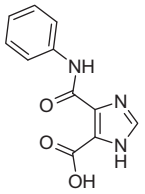

Figure 1. Compound **1**—our initial hit inhibiting the HIV-1 IN–LEDGF/p75 interaction. High-throughput random screening utilizing an AlphaScreen-based luminescence assay resulted in discovery of a novel 5-formyl-1*H*-imidazole-4-carboxamide class of allosteric IN inhibitors.

Table 1
Biological activities of 5-carbonyl-1*H*-imidazole-4-carboxamide derivatives

Compound	IN-LEDGF/p75, IC_{50}[a] (μM)	IN 3′-P, IC_{50}[b] (μM)	IN ST, IC_{50}[c] (μM)	Quench%inhibition[d]	MTT/MT-4	
					CC_{50}[e] (μM)	EC_{50}[f] (μM)
1	6 ± 4	>20	>20	<50	>20	>20
2	10 ± 2	>20	>20	<50	>20	>20
3	>20	>20	>20	<50	>20	>20
4	>20	>20	>20	<50	>20	>20
5	13 ± 3	>20	>20	<50	>20	>20
6	5.3 ± 0.6	>20	>20	<50	>20	>20
7	1.0 ± 0.3	>20	>20	<50	>20	>20
8	>20	>20	>20	<50	>20	>20
9	>20	>20	>20	<50	>20	>20
10	>20	>20	>20	<50	>20	>20
11	>20	>20	>20	<50	>20	>20
12	>20	>20	>20	<50	>20	>20
13	>20	>20	>20	<50	>20	>20
14	16 ± 10	>20	>20	<50	>20	>20
15	0.4 ± 0.1	>20	>20	<50	>20	>20
16	>20	>20	>20	<50	>20	>20

[a] Concentration required to inhibit the in vitro protein–protein interaction by 50%.
[b] Concentration required to inhibit IN 3′-processing catalysis by 50%.
[c] Concentration required to inhibit IN strand transfer catalysis by 50%.
[d] Percent inhibition exerted by compounds in quench counter-screen when tested at 20 μM.
[e] Cytotoxic concentration reducing MT-4 cell viability by 50%.
[f] Effective concentration required to reduce HIV-1 induced cytopathic effect by 50% in MT-4 cells.

and this mode of binding provided vital information for a structure-guided optimization strategy. The carboxylic moiety of **1** was shown to form two hydrogen bond (H-bond) interactions with the backbone NHs of His171 and Glu170 (Fig. 2). The phenyl ring of compound **1** packed into the hydrophobic pocket formed by IN residues Thr125, Ala128, Trp131, Trp132, and Gln168.

3.2. Initial synthesized analogues demonstrate R_1 and R_2 structural requirements

Based on our observations above, we began to design and synthesize analogues with substitutions at each terminal region of the 5-formyl-1*H*-imidazole-4-carboxamide hit scaffold (Fig. 3).

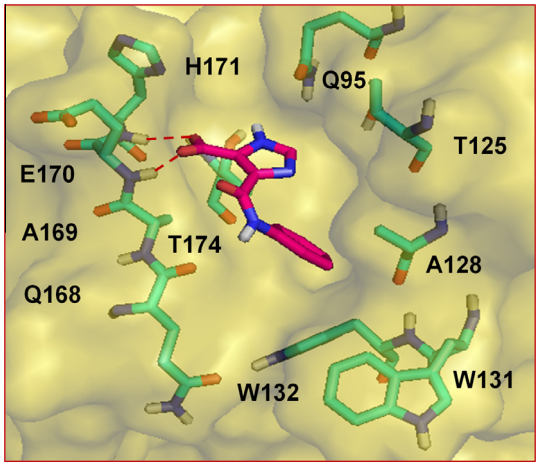

Figure 2. Compound **1** was docked onto the LEDGF/p75 binding site of IN protein in PDB 2B4J. Predicted ligand–receptor interactions included two H-bonds between the carboxylic moiety of **1** and backbone NHs of E170 and H171. Between the imidazole NH of **1** and the side chain OH of IN residue T174. Meanwhile, the phenyl ring of the ligand packed into the hydrophobic pocket occupied by LEDGF/p75 residue I365.

We designated two variable regions, with R_1 describing the original position of the terminal carboxylate hydroxyl moiety, and R_2 describing the phenyl substituent at the opposite terminus of the molecule. We first synthesized 4-((4-fluorophenyl)carbamoyl)-1*H*-imidazole-5-carboxylic acid (compound **2**) with a fluorophenyl R_2 substitution, and we found similar in vitro activity for IN-LEDGF/p75 inhibition, with an IC_{50} value of 10 ± 2 μM (Table 1). We found that an additional carbon extension of the fluorophenyl group, in our synthesized 4-((4-fluorobenzyl)carbamoyl)-1*H*-imidazole-5-carboxylic acid (compound **3**), significantly increased IC_{50} in the AlphaScreen assay above our upper measurement threshold of 20 μM (Table 1). Similarly, maintaining the original fluorophenyl R_2 substituent but replacing the R_1 hydroxyl with a methoxy in methyl 4-((4-fluorophenyl)carbamoyl)-1*H*-imidazole-5-carboxylate (compound **4**), abolished inhibitory potency to IC_{50} >20 μM (Table 1). Multiple inactive analogues that also bear a methylated R_1 moiety are displayed in Supplementary Figure 1. Compound **4** was an analogue from our in-house database and was not synthesized. These three compounds led to the conclusion that a HBA is necessary at the R_1 position, while a phenyl substituent with compact modifications is preferred at the R_2 position.

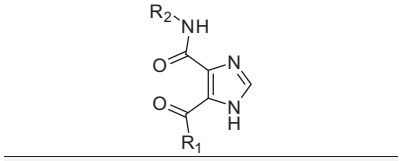

Compound	Structure	
	R_1	R_2
2	OH	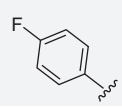
3	OH	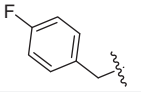
4	OCH_3	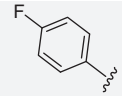
5	OH	
6	OH	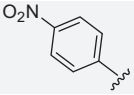
7	OH	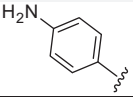

Figure 3. Initial 5-formyl-1*H*-imidazole-4-carboxamide derivatives. Two variable regions describe substitutions at the original position of the terminal carboxylate hydroxyl moiety and the phenyl substituent at the opposite terminus of the molecule.

Enhanced potency was achieved with synthesized analogues containing diverse compact R_2 phenyl modifications. Inclusion of an *ortho* nitrogen in the R_2 phenyl, generating 4-(pyridine-2-ylcarbamoyl)-1*H*-imidazole-5-carboxylic acid (compound **5**), showed acceptable activity at IC_{50} = 13 ± 3 μM (Table 1). Alternatively, a nitro- or amino-substituted phenyl ring is preferred for the R_2 structure, that is, 4-((4-nitrophenyl)carbamoyl)-1*H*-imidazole-5-carboxylic acid and 4-((4-aminophenyl)carbamoyl)-1*H*-imidazole-5-carboxylic acid (compounds **6** and **7**) showed an improved potency at IC_{50} = 5.3 ± 0.6 μM and 1.0 ± 0.3 μM, respectively (Table 1). Similar to hit compound **1**, compounds **2**–**7** were nontoxic, inactive in our quench counter-screen at the maximum dose of 20 μM, and inactive against IN catalytic activity (Table 1).

The best compound **7** was docked onto the LEDGF/p75 binding site of IN protein (PDB: 2B4J) for exploration of binding mode (Fig. 4). It displayed nearly similar binding interactions with IN as compound **1**. Specifically, the carboxylic oxygens formed H-bonds with the backbone NHs of Glu170 and His171 on IN. The imidazole NH adjacent to the carboxylic group formed an H-bond with the side chain oxygen of Thr174. The aniline group packed into the hydrophobic pocket formed by IN residues Thr125, Ala128, Trp131, Trp132, and Gln168. Figure 4 shows compound **7** docked onto IN at the LEDGF/p75 binding interface.

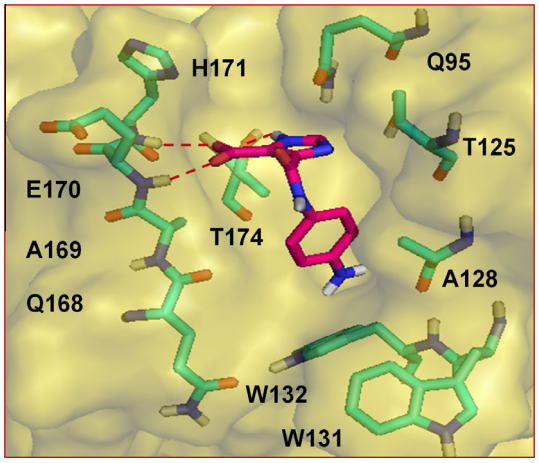

Figure 4. Compound **7** is docked onto IN protein at the IN–LEDGF/p75 interaction interface. Specific interactions included the compound's carboxylate oxygens forming hydrogen bonds with the backbone NHs of IN E170 and H171. Another hydrogen bond formed between the imidazole NH of **7** and the side chain OH of IN residue T174. The aniline group of compound **7** packed into the hydrophobic pocket formed by IN residues Thr125, Ala128, Trp131, Trp132, and Gln168.

3.3. Piperidine-based R_1 position substitutions generated inactive analogues

To explore the tolerance for extension of the HBD/HBA at the R_1 position, a panel of analogues containing piperidine-based substituents in place of the original R_1 hydroxyl group were synthesized (Fig. 5). Specifically, we prepared compounds containing morpholine, piperidin-4-ol, and piperazine R_1 moieties with either pyridine (compounds **8**–**10**, respectively) or phenol R_2 substituents (compounds **11**–**13**, respectively). Unfortunately, all of the above compounds proved inactive in our AlphaScreen assay, and were also nontoxic and inactive in our quench counter-screen and IN enzymatic assay (Table 1). Molecular docking analysis of the binding mode of these compounds may explain this lack of activity. In docking inactive compounds **8**, **9**, **11**, and **12**, we found a consistent absence of an H-bond between the compound and IN residue His171. All active compounds in this report that we studied with molecular docking exhibited this particular hydrogen bond. Conversely, inactive compounds **8**, **9**, **11**, and **12** lacked this interaction but still were predicted to form H-bonds with the backbone NH of Glu170 and packed a substituent into the hydrophobic pocket created by IN residues Thr125, Ala128, Trp131, Trp132, and Gln168. A separate panel of inactive analogues discovered during high-throughput screening of in-house analogues of compound **1** is shown in Supplementary Figure 2. These compounds did not contain piperidine-based R_1 substituents, but rather exhibited a central pyrazine in place of the original 1*H*-imidazole component. This analogue panel clearly demonstrated that the overall molecular conformation imparted by the imidazole is essential for proper in vitro activity.

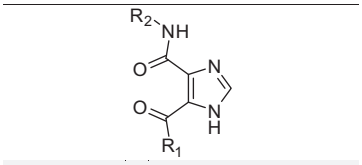

Compound	Structure	
	R_1	R_2
8	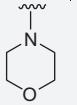	
9	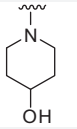	
10	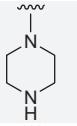	
11	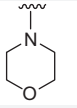	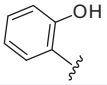
12	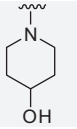	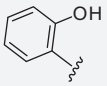
13	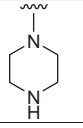	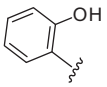

Figure 5. 5-Formyl-1*H*-imidazole-4-carboxamide analogues containing piperidine-based substituents in place of the original R_1 hydroxyl group.

3.4. Inclusion of R_1 hydrazine yielded an IN-LEDGF/p75 inhibitor with significantly increased potency

A concluding synthesis of analogues including an alternate hydrazine HBD at the R_1 position yielded encouraging results (Fig. 6). Maintaining a simple toluene as the R_2 substituent (compound **14**) gave 5-(hydrazinecarbonyl)-*N*-(*p*-tolyl)-1*H*-imidazole-4-carboxamide, which exhibited a modest IC_{50} of 16 ± 10 μM against IN-LEDGF/p75 in vitro (Table 1). However, when reverting to a pyridine R_2 component, a substantial increase in potency was observed, as 5-(hydrazinecarbonyl)-*N*-(pyridin-2-yl)-1*H*-imidazole-4-carboxamide (compound **15**) exhibited an IC_{50} value of 0.4 ± 0.1 μM (Table 1). In line with our prior observations, substitution of the hydrazine with a methylamine in N^5-methyl-N^4-(pyridine-2-yl)-1*H*-imidazole-4,5-dicarboxamide (compound **16**) abolished in vitro activity entirely (Table 1). Molecular docking analysis revealed that top compound **15** formed maximum interactions with IN (Fig. 7). Specifically, hydrogen bonds were formed between side chain and backbone NHs of His171 and both the oxygen and terminal NH at the R_1 position of compound **15**. The compound's R_1 position oxygen and carbonyl oxygen from the amide linker both formed hydrogen bonds with the backbone NH of Glu 170. While compound **15**'s pyridine moiety packed into the hydrophobic pocket formed by IN residues Thr125, Ala128, Trp131, Trp132, and Gln168, an additional hydrogen bond was formed between the compound's amide NH and the backbone oxygen of Gln168. The array of interaction points between compound **15** and IN at its interface with LEDGF/p75 may explain the compound's exceptional potency. Figure 7 shows compound **15** docked onto IN at the LEDGF/p75 binding interface. Compounds **14**–**16** all followed the trend of non-cytotoxicity in MTT assay and inactivity in our quench counter-screen or IN enzymatic assay. Unfortunately, none of the compounds detailed in this report exhibited inhibition of HIV-induced cytopathic effect in MT-4 cell culture. However, the lack of toxicity even at high doses gives us confidence that further structural optimization may hold potential for generating compounds that not only inhibit IN-LEDGF/p75 in vitro, but also during viral replication.

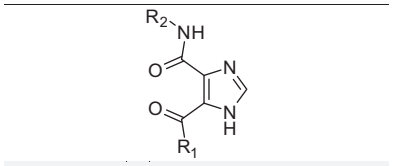

Compound	Structure	
	R_1	R_2
14	$NHNH_2$	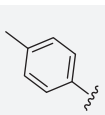
15	$NHNH_2$	
16	MeNH	

Figure 6. 5-Formyl-1*H*-imidazole-4-carboxamide analogues containing a hydrazine HBD at the R_1 position.

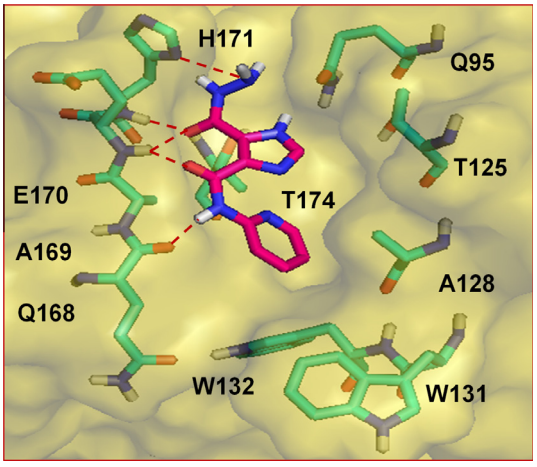

Figure 7. Compound **15** is docked onto IN protein at the IN–LEDGF/p75 interaction interface. Specific interactions included the compound forming hydrogen bonds between His171 and both the R_1 position oxygen and terminal NH, as well as between backbone NH of E170 and the oxygens of R_1 position and linker amide. The pyridine moiety of compound **15** formed a hydrophobic interaction with IN residues Thr125, Ala128, Trp131, Trp132, and Gln168, an additional hydrogen bond formed between the compound's amide NH and the backbone oxygen of Gln168.

4. Discussion

IN has to date been shown to distinctly interact with a variety of host proteins, and many of these interactions have been demonstrated to be essential for viral replication.[39,40] The majority of reported efforts to disrupt these essential interactions via rational small-molecule development have revolved around the IN-LEDGF/p75 interaction. A benzoic acid derivative known as D77[41] and a LEDGF/p75 structure-based compound named CHIBA-3003[20] were first reported to inhibit IN-LEDGF/p75 binding with low micromolar activity. Since these discoveries a series of 2-(quinolin-3-yl)acetic acid-based molecules has been rationally designed and developed to inhibit IN-LEDGF/p75 binding with reported IC_{50} values as low as 0.046 μM.[42] Though these compounds exhibited potent antiviral activity, they were shown to also evoke IN resistance mutations, namely the A128T substitution.[22] However, recent reports demonstrate that the promotion of IN multimerization by these so-called LEDGINs or ALLINIs plays a significant, if not more important, role in ultimately inhibiting viral replication.[43–46] All of this work has revealed not only that inhibitors of IN-LEDGF/p75 can be successful at allosteric IN inhibition leading to antiviral activity, but also that there is a necessity for discovering novel inhibitory structural scaffolds.

Here we present a novel panel of 5-carbonyl-1*H*-imidazole-4-carboxamide inhibitors of the IN–LEDGF/p75 interaction with our best compound exhibiting submicromolar activity. This class of compounds has not been previously developed in antiviral research, and the structural scaffold significantly differs from all prior IN-LEDGF/p75 inhibitors. Thus, we anticipate a divergent viral resistance profile to emerge in response to in vivo drug pressure. All of the compounds reported in this study were non-toxic in a human cell line and lacked allosteric inhibition of IN enzymatic activity. Though the compounds reported herein did not achieve antiviral effects in vitro, our work here illustrates the power of rational compound optimization following high-throughput random screening, and lends credence to the belief that such advances can be accomplished in the academic realm. Our active compounds have not been previously reported, though the central scaffold has been described by our group for targeting the HIV-1 IN catalytic site.[35] Specifically, 4-((2-benzoyl-4-bromophenyl)carbamoyl)-1*H*-imidazole-5-carboxylic acid (Supplementary Fig. 1, S15), containing a benzophenoneamide at the R_2 position, exhibited 16 and 17 μM activity against 3′-processing and strand transfer, respectively. This compound contained considerably more bulk at the R_2 position than our top leads, which may have lent additional binding specificity to the IN active site over the IN-LEDGF/p75 interfacial hotspot. On the other hand, this particular molecule may not be binding to the IN catalytic site at all, but rather allosterically inhibiting enzymatic activity. Investigation of the binding mode of this and other analogous compounds with IN is ongoing in our laboratory.

Aside from targeting IN, analogous compounds to our 5-carbonyl-1*H*-imidazole-4-carboxamides have been described as modulators of JAK-2[47] and characterized for their antiproliferative and antituberculosis activity.[48,49] The fact that such closely related compounds can exhibit broad activity profiles underscores the importance of selectivity monitoring during the development process. Though none of our reported analogues exhibited cytotoxicity in MTT assay, the potential for off-target effects with this class of compounds is apparent. However, the formulations of these 5-carbonyl-1*H*-imidazole-4-carboxamides are optimal for clinical development, and distinctive functional groups on our core scaffold can be further optimized. Structure–activity analysis yielded strict structural requirements for in vitro potency that included a HBA/HBD presence at the R_1 position, a central imidazole substituent, and a more lax phenyl-based R_2 requirement. Our future synthetic strategy will exploit these findings with the hope of enhancing the antiviral potency of these inhibitors while still maintaining their nontoxic profile.

5. Conclusions

From an initial high-throughput screening program, we identified 4-(phenylcarbamoyl)-1*H*-imidazole-5-carboxylic acid as a potent and selective inhibitor of the in vitro interaction between HIV-1 IN and LEDGF/p75. Molecular docking guided a structure-based chemical synthesis that ultimately yielded a class of nontoxic 5-carbonyl-1*H*-imidazole-4-carboxamide inhibitors of the above interaction with submicromolar IC_{50} values. Though our top compounds did not exhibit antiviral activity in MT-4 cells, favorable interactions with IN residues essential for the LEDGF/p75 interaction were predicted. Work is ongoing in our laboratory to optimize the chemical properties of our top compounds toward more potent inhibition of HIV-1 replication in cell culture.

6. Experimental section

6.1. Expression and purification of recombinant HIV-1 integrase and LEDGF/p75 proteins

The plasmids for His-IN, GST-IN, and LEDGF/p75 were expressed in *Escherichia coli* BL21(De3) pLysS expression strain (Invitrogen) after induction by IPTG (1 mM) at 0.75 optical density absorbance (595 nm). The culture was grown for an additional 3–4 h at 37 °C, followed by centrifugation at 3000 rpm in a bucket rotor centrifuge (Beckman) for 20 min. Cell lysis, Ni-affinity chromatography purification, and dialysis were performed as detailed in.[50]

6.2. IN-LEDGF/p75 AlphaScreen assay and emission quench AlphaScreen assay

The AlphaScreen assay was performed according to the manufacturer's protocol (PerkinElmer, Benelux). Reactions were performed in a 25 μl final volume in 384-well Optiwell™ microtiter plates (PerkinElmer). The reaction buffer contained 25 mM Tris–HCl (pH 7.4), 150 mM NaCl, 1 mM $MgCl_2$, 0.01% (v/v) Tween-20

and 0.1% (w/v) bovine serum albumin. His6-tagged integrase (300 nM final concentration) was incubated with compound at a final concentration of 20 μM for 30 min at 4 °C. FLAG-tagged LEDGF/p75 protein was then added at 300 nM final concentration, and the reaction was incubated for an additional 60 min at 4 °C. Subsequently, 5 μL Ni-chelate-coated donor beads and 5 μL anti-FLAG antibody coated acceptor beads were added to a final concentration of 20 μg/mL of both beads. Proteins and beads were incubated for 1 h at 30 °C in order to allow association to occur. Exposure of the reaction to direct light was omitted as much as possible and the emission of light from the acceptor beads was measured in the EnVision plate reader (PerkinElmer) and analyzed using the EnVision manager software. The emission quench AlphaScreen assay was carried out identically to the IN-LEDGF/p75 AlphaScreen assay, except instead of the IN and LEDGF/p75 proteins, a FLAG-tagged GST construct was added at a final concentration of 500 nM.

6.3. Drug susceptibility assays

The inhibitory effect of antiviral drugs on the HIV-induced cytopathic effect in MT-4 cell culture was determined by the MTT assay as previously described.[22]

6.4. Molecular docking

Select compounds were docked in the LEDGF binding site of HIV-1 IN (PDB ID: 2B4J) using GOLD (Genetic Optimization for Ligand Docking) software package, version 4.0 (Cambridge Crystallographic Data Centre, Cambridge, UK). Prior to docking, compounds were energy-minimized, and all possible combinations of stereoisomers and conformers were generated with LigPrep from Schrodinger using the OPLS-2005 force field.[51] Within LigPrep, Epik module was used to generate all possible ionization forms of ligands at pH 7.0 ± 0.2. GOLD uses a genetic algorithm to explore the conformational space of a compound inside the binding site of a protein.[52,53] Docking studies were performed using the standard default settings with 100 genetic algorithm (GA) runs on each molecule. For each of the 100 independent GA runs, a maximum of 100,000 operations was performed on a set of five groups with a population of 100 individuals. With respect to ligand flexibility, special care was taken by including options such as flipping of ring corners, amides, pyramidal nitrogens, secondary and tertiary amines, and rotation of carboxylate groups, as well as torsion angle distribution and post-process rotatable bonds as default. The annealing parameters were used as default cutoff values of 3.0 Å for hydrogen bonds and 4.0 Å for van der Waals interactions. Hydrophobic fitting points were calculated to facilitate the correct starting orientation of the compound for docking by placing the hydrophobic atoms appropriately in the corresponding areas of the active site. When the top three solutions attained root-mean-square deviation (rmsd) values within 1.5 Å, docking was terminated. GOLD-Score, a scoring function within the software, is a dimensionless fitness value that takes into account the intra- and intermolecular hydrogen bonding interaction energy, van der Waals energy, and ligand torsion energy.[52,53]

6.5. General synthetic methods

Starting materials, reagents and solvents were purchased from commercial suppliers and were used without further purification. THF and CH_2Cl_2 were dried by anhydrous sodium sulfate before used. Analytical thin-layer chromatography (TLC) was performed on silica gel (GF-254) plates. Visualization was effected with ultraviolet light or iodine vapor. NMR spectra were recorded on a Varian Mercury 300 or 400 MHz spectrometer. The data are reported in parts per million relative to TMS and referenced to the solvent in which they were run. ESI-MS spectra were recorded on a Finnigan LCQ Deca mass spectrometer. Liquid chromatography–mass spectrometry (LC–MS) was carried out on Waters Micromass ZQ2000.

6.5.1. Diphenyl 5,10-dioxo-5,10-dihydrodiimidazo[1,5-*a*:1′,5′-*d*]pyrazine-1,6-dicarboxylate (17)

To a solution of imidazole-4,5-dicarboxylic acid (400 mg, 2.56 mmol) in 5 mL of toluene was added 1.12 mL of thionyl chloride (15.38 mmol) and 0.1 mL of DMF at rt. The reaction mixture was stirred at 90 °C for 16 h. Then 5 mL of DCM was added to the suspension and the solvent was removed by evaporation. This process was repeated twice. The resulting acid chloride was dissolved in 10 mL of DCM and cooled to 0 °C. Phenol (2.82 mmol) in 5 mL of DCM was added and the resulting solution was stirred at 0 °C for 1 h. Then the solid product was collected by vacuum filtration, washed with 10 mL of DCM twice, and dried under vacuum to yield 0.632 g of crude product **17** (83.6% over two steps) as a tan solid. ^{1}H NMR (300 Hz, DMSO) δ 9.12 (s, 2H), 7.52–7.56 (m, 4H), 7.34–7.40 (m, 6H); ESI-MS: 429 $[M+1]^+$.

6.5.2. General procedure for the preparation of amide-ester 18a–c. Method A

To a solution of **17** (100 mg, 0.233 mmol) in 30 mL of dry THF was added 2-aminopyridine (30.8 mg, 0.328 mmol) in 2 mL of THF dropwise over 2 min at 0 °C. The ice bath was removed after 10 min, and the solution was stirred at rt for 18 h. The solvent was removed under vacuum, and the residue was purified by column chromatography on silica gel to give a white solid **18a** (84.9 mg, 84% yield). ^{1}H NMR (400 MHz, $CDCl_3$) δ 12.37 (s, 1H), 11.52 (s, 1H), 8.40 (d, J = 3.9 Hz, 1H), 8.31 (d, J = 8.4 Hz, 1H), 7.95 (s, 1H), 7.80–7.72 (m, 1H), 7.46 (t, J = 7.9 Hz, 2H), 7.33 (d, J = 9.2 Hz, 2H), 7.29 (s, 1H), 7.11 (dd, J = 7.1, 5.0 Hz, 1H). ESI-MS: 308 $[M+1]^+$.

6.5.3. Phenyl 4-(*p*-tolylcarbamoyl)-1*H*-imidazole-5-carboxylate (18b)

The title compound was obtained from **17** (100 mg, 0.233 mmol) and *p*-toluidine (49.9 mg, 0.466 mmol) as described above in the method A. Pale yellow solid, yield 78%. ^{1}H NMR (300 MHz, $CDCl_3$) δ 11.62 (s, 1H), 8.32 (d, J = 8.0 Hz, 1H), 7.64 (d, J = 6.3, 2H), 7.46–7.23 (m, 7H), 2.32 (s, 3H). EI-MS: 321.3 $[M]^+$.

6.5.4. Phenyl 4-((2-(benzyloxy)phenyl)carbamoyl)-1*H*-imidazole-5-carboxylate (18c)

The title compound was obtained from **17** (100 mg, 0.233 mmol) and 2-(benzyloxy)aniline (92.7 mg, 0.466 mmol) as described above in the method A. Pale yellow solid, yield 81%. ^{1}H NMR (300 MHz, $CDCl_3$) δ 11.88 (s, 1H), 8.32 (d, J = 8.0 Hz, 1H), 7.88 (s, 1H), 7.46–7.38 (m, 2H), 7.37–7.27 (m, 3H), 7.24–7.13 (m, 5H), 7.12–7.08 (m, 1H), 7.04–6.97 (m, 2H), 5.09 (s, 2H). EI-MS: 413.2 $[M]^+$.

6.5.5. General procedure for the preparation of acid-amide 2, 3, 5–7. Method B. 4-((4-Fluorophenyl)carbamoyl)-1*H*-imidazole-5-carboxylic acid (2)

To a solution of **17** (100 mg, 0.233 mmol) in 30 mL of dry THF was added *p*-fluoroaniline (51.7 mg, 0.466 mmol) in 2 mL THF dropwise over 2 min at 0 °C. The ice bath was removed after 10 min, and the solution was stirred at rt for 18 h. Solvent was removed by concentrating under vacuum. The residue was dissolved in 5 mL of methanol and the potassium hydroxide (200 mg, 3.57 mmol) was added to this suspension at 0 °C. The ice bath was removed after 10 min, and the solution was

continuously stirred at rt for 8 h. Then the crude product was precipitated out when the pH was adjusted to 5 with 3 N HCl. The solid was filtered and subsequently recrystallized from methanol and ethyl acetate to give pale yellow solid **2**, in an overall yield of 68% for two steps. ^{1}H NMR (300 MHz, DMSO-d_6) δ 8.223 (s, 1H), 7.808 (d, J = 9.0, 2H), 7.256 (d, J = 9.0, 2H); ESI-MS: 250 $[M+1]^+$; HRESI-MS: m/z calcd for $C_{11}H_9FN_3O_3$ ($[M+H]^+$) 250.1979; found 250.1983.

6.5.6. 4-((4-Fluorobenzyl)carbamoyl)-1*H*-imidazole-5-carboxylic acid (3)

The title compound was obtained from **17** (100 mg, 0.233 mmol) and *p*-fluorobenzylamine (58.3 mg, 0.466 mmol) as described above in the method B. Pale yellow solid, yield 62%; ^{1}H NMR (300 MHz, DMSO-d_6) δ 8.060 (s, 1H), 7.363 (d, J = 7.8, 2H), 7.162 (d, J = 7.8, 2H), 4.494 (s, 2H); ESI-MS: 264 $[M+1]^+$; HRESI-MS: m/z calcd for $C_{12}H_{11}FN_3O_3$ ($[M+H]^+$) 264.2245; found 264.2238.

6.5.7. 4-(Pyridin-2-ylcarbamoyl)-1*H*-imidazole-5-carboxylic acid (5)

The title compound was obtained from **17** (100 mg, 0.233 mmol) and 2-aminopyridine (84 mg, 0.466 mmol) as described above in the method B. Pale yellow solid, yield 67%; ^{1}H NMR (300 MHz, DMSO-d_6) δ 8.281(s, 1H), 7.844(d, J = 11.7, 2H), 7.411(d, J = 11.7, 2H); ^{13}C NMR (100 MHz, DMSO-d_6) δ 160.4, 150.7, 148.4, 138.5, 137.6, 137.5, 135.6, 129.8, 120.5, 114.4; ESI-MS: 233 $[M+1]^+$; HRESI-MS: m/z calcd for $C_{10}H_9N_4O_3$ ($[M+H]^+$) 233.0675; found 233.0690.

6.5.8. 4-((4-Nitrophenyl)carbamoyl)-1*H*-imidazole-5-carboxylic acid (6)

The title compound was synthesized from **17** (100 mg, 0.233 mmol) and *p*-nitroaniline (64.4 mg, 0.466 mmol) as described above in the method B. Pale yellow solid, yield 61%; ^{1}H NMR (300 MHz, DMSO-d_6) δ 8.298(s, 1H), 7.861(d, J = 9.0, 2H), 7.427(d, J = 9.0, 2H); ESI-MS: 277 $[M+1]^+$; HRESI-MS: m/z calcd for $C_{11}H_9N_4O_5$ ($[M+H]^+$) 277.1331; found 277.1318.

6.5.9. 4-((4-Aminophenyl)carbamoyl)-1*H*-imidazole-5-carboxylic acid (7)

The title compound was synthesized from **17** (100 mg, 0.233 mmol) and (9*H*-fluoren-9-yl)methyl (4-aminophenyl)carbamate (153.8 mg, 0.466 mmol) as described above in the method B. Pale yellow solid, yield 72%; ^{1}H NMR (300 MHz, DMSO-d_6) δ 8.362 (s, 1H), 8.267(d, J = 9.1, 1H), 7.804 (m, 2H), 7.106 (dd, J = 5.4, 6.0, 1H); ^{13}C NMR (100 MHz, DMSO-d_6) δ 161.22, 159.91, 137.68, 136.25, 133.12, 129.23, 127.93, 123.25, 122.44; ESI-MS: 247 $[M+1]^+$; HRESI-MS: m/z calcd for $C_{11}H_{11}N_4O_3$ ($[M+H]^+$) 247.0831; found 247.0815.

6.5.10. General procedure for the preparation of unsymmetric 4,5-dicarboxamide 8 and 10. Method C. 5-(Morpholine-4-carbonyl)-*N*-(pyridin-2-yl)-1*H*-imidazole-4-carboxamide (8)

Morpholine (18.6 mg, 0.213 mmol) and **18a** (60 mg, 0.194 mmol) in DMF (3.0 mL) were heated to 130 °C for 30 min in a CEM microwave oven. The reaction was allowed to cool and the DMF was removed under vacuum, the residue was purified by column chromatography on silica gel to give a white solid 47.3 mg, (yield: 81%): ^{1}H NMR (300 MHz, $CDCl_3$) δ 13.51 (s, 1H), 12.67 (s, 1H), 8.37 (d, J = 4.9 Hz, 1H), 8.23 (d, J = 8.4 Hz, 1H), 7.96 (s, 1H), 7.91–7.81 (m, 1H), 7.16 (dd, J = 6.8, 5.4 Hz, 1H), 3.82–3.68 (m, 4H), 3.68–3.59 (m, 2H), 3.40–3.28 (m, 2H). ESI-MS: 302.3 $[M+1]^+$; HRESI-MS: m/z calcd for $C_{14}H_{16}N_5O_3$ ($[M+H]^+$) 302.1253; found 302.1264.

6.5.11. 5-(4-Hydroxypiperidine-1-carbonyl)-*N*-(pyridin-2-yl)-1*H*-imidazole-4-carboxamide (9)

Piperidin-4-yl acetate (27.7 mg, 0.213 mmol) and **18a** (60 mg, 0.194 mmol) in DMF (3.0 mL) were heated to 130 °C for 30 min in a CEM microwave oven. The reaction mixture was allowed to rt and the DMF was removed under vacuum. The residue was dissolved in 1 N LiOH (2 mL) and THF (2 mL). The solution was stirred at rt for 6 h. After the reaction was completed, the pH of the aqueous phase was adjusted to 3 and was extracted with DCM (10 mL × 2). The DCM was removed under vacuum, the residue was purified by column chromatography on silica gel to give a white solid 40.9 mg, (yield: 67% in two steps): ^{1}H NMR (300 MHz, $CDCl_3$) δ 13.44 (s, 1H), 12.91–12.25 (s, 1H), 8.37 (d, J = 4.2 Hz, 1H), 8.22 (d, J = 8.3 Hz, 1H), 7.94 (s, 1H), 7.85 (t, J = 7.8 Hz, 1H), 7.21–7.12 (m, 1H), 4.85–4.76 (m, 1H), 4.15–4.03 (m, 1H), 3.86–3.73 (m, 1H), 3.42–3.27 (m, 4H), 1.95–1.68 (m, 2H), 1.54–1.29 (m, 2H). ESI-MS: 316.2 $[M+1]^+$; HRESI-MS: m/z calcd for $C_{15}H_{18}N_5O_3$ ($[M+H]^+$) 316.1410; found 316.1400.

6.5.12. 5-(Piperazine-1-carbonyl)-*N*-(pyridin-2-yl)-1*H*-imidazole-4-carboxamide (10)

The title compound was obtained from **18a** (100 mg, 0.233 mmol) and piperazine (38.4 mg, 0.466 mmol) as described above in the method C. white solid, yield 87%; ^{1}H NMR (300 MHz, $CDCl_3$) δ 8.37 (d, J = 3.9 Hz, 1H), 8.22 (d, J = 8.4 Hz, 1H), 7.94 (s, 1H), 7.85 (t, J = 7.7 Hz, 1H), 7.21–7.12 (m, 1H), 3.90–3.73 (m, 2H), 3.70–3.60 (m, 2H), 2.85–2.76 (m, 2H), 2.76–2.68 (m, 2H). ESI-MS: 301.2 $[M+1]^+$; HRESI-MS: m/z calcd for $C_{14}H_{17}N_6O_2$ ($[M+H]^+$) 301.1413; found 301.1417.

6.5.13. *N*-(2-Hydroxyphenyl)-5-(morpholine-4-carbonyl)-1*H*-imidazole-4-carboxamide (11)

Morpholine (18.6 mg, 0.213 mmol) and **18c** (80 mg, 0.194 mmol) in DMF (3.0 mL) were heated to 130 °C for 30 min in a CEM microwave oven. The reaction was allowed to cool and the DMF was removed under vacuum. The residue was dissolved in EtOH (5 mL) and 10 percent 20% $Pd(OH)_2$/C was added thereto. The reaction mixture was stirred at rt for 3 h under hydrogen atmosphere. After completion of the reaction, the solution was filtered with a cellite and the filtrate was distilled under a reduced pressure to afford the title compound, which was purified by column chromatography on silica gel to give a white solid 46.7 mg, (yield: 76.1% in two steps): ^{1}H NMR (300 MHz, $CDCl_3$) δ 8.02–7.95 (m, 1H), 7.81 (s, 1H), 7.00–6.95 (m, 1H), 6.86 (t, J = 1.4 Hz, 1H), 6.84–6.80 (m, 1H), 3.84–3.75 (m, 4H), 3.73–3.64 (m, 4H). ESI-MS: 317.2 $[M+1]^+$; HRESI-MS: m/z calcd for $C_{15}H_{17}N_4O_4$ ($[M+H]^+$) 317.1250; found 317.1255.

6.5.14. *N*-(2-Hydroxyphenyl)-5-(4-hydroxypiperidine-1-carbonyl)-1*H*-imidazole-4-carboxamide (12)

Piperidin-4-yl acetate (27.7 mg, 0.213 mmol) and **18c** (80 mg, 0.194 mmol) in DMF (3.0 mL) were heated to 130 °C for 30 min in a CEM microwave oven. The reaction was allowed to cool and the DMF was removed under vacuum. The residue was dissolved in 1 N LiOH (2 mL) and THF (2 mL). The solution was stirred at rt. After the reaction was completed, the pH of the aqueous phase was adjusted to 3 and was extracted with DCM (10 mL × 2). The combined organic phases were evaporated in vacuum, and the residue was dissolved in EtOH (5 mL). 10 percent 20% $Pd(OH)_2$/C was added thereto, and the reaction mixture was stirred at rt for 3 h under hydrogen atmosphere. After completion of the reaction, the resulting solution was filtered with a cellite and distilled under a reduced pressure to obtain the title compound, which was purified by column chromatography on silica gel to give a white solid 36.2 mg, (yield: 56.7% in three steps): ^{1}H NMR (300 MHz, $CDCl_3$) δ 8.31–8.09 (m, 1H), 7.87 (s, 1H), 7.01–6.87 (m, 2H), 6.85–6.76 (m, 1H), 4.80 (s, 1H), 4.09 (s, 1H), 3.77 (s, 1H), 3.38–3.29 (m, 4H),

1.89–1.59 (m, 2H), 1.51–1.26 (m, 2H). ESI-MS: 331.1 $[M+1]^+$; HRES-I-MS: *m/z* calcd for $C_{16}H_{18}N_4O_4Na$ ($[M+Na]^+$) 353.1226; found 353.1214.

6.5.15. *N*-(2-Hydroxyphenyl)-5-(piperazine-1-carbonyl)-1*H*-imidazole-4-carboxamide (13)

The title compound was prepared from **18c** (80 mg, 0.194 mmol) and piperazine (18.3 mg, 0.213 mmol) with a procedure similar to that for **11**. White solid, yield 61%; ^{1}H NMR (300 MHz, $CDCl_3$) δ 8.18 (d, J = 7.5 Hz, 1H), 7.86 (s, 1H), 6.98–6.87 (m, 2H), 6.84–6.77 (m, 1H), 3.65–3.48 (m, 4H), 2.81–2.72 (m, 2H), 2.72–2.62 (m, 2H). ESI-MS: 316.1 $[M+1]^+$; HRESI-MS: *m/z* calcd for $C_{15}H_{18}N_5O_3$ ($[M+H]^+$) 316.1410; found 316.1421.

6.5.16. General procedure for the preparation of unsymmetric 4,5-dicarboxamide 14–16. Method D. 5-(Hydrazinecarbonyl)-*N*-(*p*-tolyl)-1*H*-imidazole-4-carboxamide (14)

To a solution of **18b** (100 mg, 0.164 mmol) in 30 mL of dry THF was added 0.1 mL of hydrazine hydrate (85%) at 0 °C. The ice bath was removed after 10 min, and the solution was stirred at 50 °C overnight, the solid was filtered. The filtrate was concentrated under vacuum to yield a solid that was crystallized and subsequently recrystallized from methanol and ethyl acetate. The final product was dried under vacuum to give 25 mg of **14** in an overall yield of 64% for two steps; White solid; ^{1}H NMR (300 MHz, DMSO-d_6) δ 8.027 (s, 1H), 7.607 (d, J = 6.3, 2H), 7.206 (d, J = 6.3, 2H), 2.298 (s, 3H); ^{13}C NMR (100 MHz, DMSO-d_6) δ 162.9, 156.3, 137.2, 136.4, 135.6, 134.2, 133.2, 130.0, 129.6, 121.7, 119.8, 21.0; ESI-MS: 260 $[M+1]^+$; HRESI-MS: *m/z* calcd for $C_{12}H_{14}N_5O_2$ ($[M+H]^+$) 260.1069; found 260.1074.

6.5.17. 5-(Hydrazinecarbonyl)-*N*-(pyridin-2-yl)-1*H*-imidazole-4-carboxamide (15)

The title compound was prepared from **18a** (80 mg, 0.194 mmol) as described above in the method D. White solid, yield 62%; ^{1}H NMR (300 MHz, DMSO-d_6) δ 8.363 (d, J = 4.8, 1H), 8.251 (d, J = 8.4, 1H), 7.941 (s, 1H), 7.841 (dd, J = 4.8, 8.4, 1H), 7.152 (dd, J = 4.8, 8.4, 1H); ^{13}C NMR (100 MHz, DMSO-d_6) δ 163.5, 160.5, 153.2, 148.0, 137.7, 134.9, 133.5, 132.2, 118.6, 114.0; ESI-MS: 247 $[M+1]^+$; HRESI-MS: *m/z* calcd for $C_{10}H_{11}N_6O_2$ ($[M+H]^+$) 247.2254; found 247.2259.

6.5.18. N^5-Methyl-N^4-(*p*-tolyl)-1*H*-imidazole-4,5-dicarboxamide (16)

The title compound was prepared from **18a** (80 mg, 0.194 mmol) as described above in the method D, in which 30% methylamine aqueous solution was used to replace 85% hydrazine hydrate. White solid, yield 66% for two steps. ^{1}H NMR (300 MHz, DMSO-d_6) δ 8.385 (d, J = 4.8, 1H), 8.270 (d, J = 8.4, 1H), 7.972 (s, 1H), 7.856 (dd, J = 4.8, 8.4, 1H), 7.170 (dd, J = 4.8, 8.4, 1H), 2.871 (d, J = 4.5, 3H); ^{13}C NMR (100 MHz, DMSO-d_6) δ 166.0, 159.4, 154.1, 150.7, 140.7, 139.5, 135.8, 130.2, 122.2, 116.2, 28.4; ESI-MS: 246 $[M+1]^+$; HRESI-MS: *m/z* calcd for $C_{11}H_{12}N_5O_2$ ($[M+H]^+$) 246.0991; found 246.1003.

Acknowledgments

We thank Dr. Jae Jung for providing us with the FLAG-GST plasmid and Gabriel Franco and Gustavo Carvalho for assistance with high-throughput screening. This work was supported by an NIH/NIAID (R21 AI081610) grant, a research grant from the Campbell foundation (N.N.), and a National Natural Science Foundation of China (81072527, 81021062, Y.Q.L.).

Supplementary data

Supplementary data associated with this article can be found, in the online version, at http://dx.doi.org/10.1016/j.bmc.2013.07.047.

References and notes

1. Qian, K.; Morris-Natschke, S. L.; Lee, K. H. *Med. Res. Rev.* **2009**, *29*, 369.
2. El Safadi, Y.; Vivet-Boudou, V.; Marquet, R. *Appl. Microbiol. Biotechnol.* **2007**, *75*, 723.
3. Temesgen, Z.; Warnke, D.; Kasten, M. J. *Expert Opin. Pharmacother.* **2006**, *7*, 1541.
4. Nguyen, B. Y.; Isaacs, R. D.; Teppler, H.; Leavitt, R. Y.; Sklar, P.; Iwamoto, M.; Wenning, L. A.; Miller, M. D.; Chen, J.; Kemp, R.; Xu, W.; Fromtling, R. A.; Vacca, J. P.; Young, S. D.; Rowley, M.; Lower, M. W.; Gottesdiener, K. M.; Hazuda, D. J. *Ann. N.Y. Acad. Sci.* **2011**, *1222*, 83.
5. Summa, V.; Petrocchi, A.; Bonelli, F.; Crescenzi, B.; Donghi, M.; Ferrara, M.; Fiore, F.; Gardelli, C.; Gonzalez Paz, O.; Hazuda, D. J.; Jones, P.; Kinzel, O.; Laufer, R.; Monteagudo, E.; Muraglia, E.; Nizi, E.; Orvieto, F.; Pace, P.; Pescatore, G.; Scarpelli, R.; Stillmock, K.; Witmer, M. V.; Rowley, M. *J. Med. Chem.* **2008**, *51*, 5843.
6. Ramkumar, K.; Neamati, N. *Core Evid.* **2010**, *4*, 131.
7. Serrao, E.; Odde, S.; Ramkumar, K.; Neamati, N. *Retrovirology* **2009**, *6*, 25.
8. Kobayashi, M.; Nakahara, K.; Seki, T.; Miki, S.; Kawauchi, S.; Suyama, A.; Wakasa-Morimoto, C.; Kodama, M.; Endoh, T.; Oosugi, E.; Matsushita, Y.; Murai, H.; Fujishita, T.; Yoshinaga, T.; Garvey, E.; Foster, S.; Underwood, M.; Johns, B.; Sato, A.; Fujiwara, T. *Antiviral Res.* **2008**, *80*, 213.
9. Nakahara, K.; Wakasa-Morimoto, C.; Kobayashi, M.; Miki, S.; Noshi, T.; Seki, T.; Kanamori-Koyama, M.; Kawauchi, S.; Suyama, A.; Fujishita, T.; Yoshinaga, T.; Garvey, E. P.; Johns, B. A.; Foster, S. A.; Underwood, M. R.; Sato, A.; Fujiwara, T. *Antiviral Res.* **2009**, *81*, 141.
10. Potter, S. J.; Lemey, P.; Dyer, W. B.; Sullivan, J. S.; Chew, C. B.; Vandamme, A. M.; Dwyer, D. E.; Saksena, N. K. *Virology* **2006**, *348*, 35.
11. Collier, A. C.; Coombs, R. W.; Fischl, M. A.; Skolnik, P. R.; Northfelt, D.; Boutin, P.; Hooper, C. J.; Kaplan, L. D.; Volberding, P. A.; Davis, L. G.; Henrard, D. R.; Weller, S.; Corey, L. *Ann. Intern. Med.* **1993**, *119*, 786.
12. Collier, A. C.; Coombs, R. W.; Schoenfeld, D. A.; Bassett, R.; Baruch, A.; Corey, L. *Antiviral Res.* **1996**, *29*, 99.
13. Collier, A. C. *Adv. Exp. Med. Biol.* **1996**, *394*, 355.
14. Al-Mawsawi, L. Q.; Neamati, N. *ChemMedChem* **2011**, *6*, 228.
15. Cherepanov, P.; Maertens, G.; Proost, P.; Devreese, B.; Van Beeumen, J.; Engelborghs, Y.; De Clercq, E.; Debyser, Z. *J. Biol. Chem.* **2003**, *278*, 372.
16. Hombrouck, A.; De Rijck, J.; Hendrix, J.; Vandekerckhove, L.; Voet, A.; De Maeyer, M.; Witvrouw, M.; Engelborghs, Y.; Christ, F.; Gijsbers, R.; Debyser, Z. *PLoS Pathog.* **2007**, *3*, e47.
17. De Rijck, J.; Vandekerckhove, L.; Gijsbers, R.; Hombrouck, A.; Hendrix, J.; Vercammen, J.; Engelborghs, Y.; Christ, F.; Debyser, Z. *J. Virol.* **2006**, *80*, 11498.
18. Cherepanov, P.; Devroe, E.; Silver, P. A.; Engelman, A. *J. Biol. Chem.* **2004**, *279*, 48883.
19. Rahman, S.; Lu, R.; Vandegraaff, N.; Cherepanov, P.; Engelman, A. *Virology* **2007**, *357*, 79.
20. De Luca, L.; Barreca, M. L.; Ferro, S.; Christ, F.; Iraci, N.; Gitto, R.; Monforte, A. M.; Debyser, Z.; Chimirri, A. *ChemMedChem* **2009**, *4*, 1311.
21. De Luca, L.; Ferro, S.; Gitto, R.; Barreca, M. L.; Agnello, S.; Christ, F.; Debyser, Z.; Chimirri, A. *Bioorg. Med. Chem.* **2010**, *18*, 7515.
22. Christ, F.; Voet, A.; Marchand, A.; Nicolet, S.; Desimmie, B. A.; Marchand, D.; Bardiot, D.; Van der Veken, N. J.; Van Remoortel, B.; Strelkov, S. V.; De Maeyer, M.; Chaltin, P.; Debyser, Z. *Nat. Chem. Biol.* **2010**, *6*, 442.
23. Wiznycia, A. V.; Baures, P. W. *J. Org. Chem.* **2002**, *67*, 7151.
24. Wiznycia, A. V.; Rush, J. R.; Baures, P. W. *J. Org. Chem.* **2004**, *69*, 8489.
25. http://www.drugbank.ca.
26. http://clinicaltrials.gov/.
27. http://toxnet.nlm.nih.gov/.
28. http://www.ehso.com/carcinogens.php.
29. http://potency.berkeley.edu.
30. http://www.oehha.ca.gov/prop65/prop65_list/Newlist.html.
31. http://www.asinex.com.
32. http://www.enamine.net.
33. http://vitasmlab.com.
34. Dayam, R.; Sanchez, T.; Clement, O.; Shoemaker, R.; Sei, S.; Neamati, N. *J. Med. Chem.* **2005**, *48*, 111.
35. Dayam, R.; Sanchez, T.; Neamati, N. *J. Med. Chem.* **2005**, *48*, 8009.
36. Dayam, R.; Sanchez, T.; Neamati, N. *ChemMedChem* **2006**, *1*, 238.
37. Serrao, E.; Debnath, B.; Otake, H.; Kuang, Y.; Christ, F.; Debyser, Z.; Neamati, N. *J. Med. Chem.* **2013**, *56*, 2311.
38. Christ, F.; Shaw, S.; Demeulemeester, J.; Desimmie, B. A.; Marchand, A.; Butler, S.; Smets, W.; Chaltin, P.; Westby, M.; Debyser, Z.; Pickford, C. *Antimicrob. Agents Chemother.* **2012**, *56*, 4365.
39. Van Maele, B.; Debyser, Z. *AIDS Rev.* **2005**, *7*, 26.
40. Al-Mawsawi, L. Q.; Neamati, N. *Trends Pharmacol. Sci.* **2007**, *28*, 526.
41. Du, L.; Zhao, Y.; Chen, J.; Yang, L.; Zheng, Y.; Tang, Y.; Shen, X.; Jiang, H. *Biochem. Biophys. Res. Commun.* **2008**, *375*, 139.
42. Rouet, R.; Lowe, D.; Dudgeon, K.; Roome, B.; Schofield, P.; Langley, D.; Andrews, J.; Whitfeld, P.; Jermutus, L.; Christ, D. *Nat. Protoc.* **2012**, *7*, 364.

43. Kessl, J. J.; Jena, N.; Koh, Y.; Taskent-Sezgin, H.; Slaughter, A.; Feng, L.; de Silva, S.; Wu, L.; Le Grice, S. F.; Engelman, A.; Fuchs, J. R.; Kvaratskhelia, M. *J. Biol. Chem.* **2012**, *287*, 16801.
44. Jurado, K. A.; Wang, H.; Slaughter, A.; Feng, L.; Kessl, J. J.; Koh, Y.; Wang, W.; Ballandras-Colas, A.; Patel, P. A.; Fuchs, J. R.; Kvaratskhelia, M.; Engelman, A. *Proc. Natl. Acad. Sci. U.S.A.* **2013**, *110*, 8690.
45. Feng, L.; Sharma, A.; Slaughter, A.; Jena, N.; Koh, Y.; Shkriabai, N.; Larue, R. C.; Patel, P. A.; Mitsuya, H.; Kessl, J. J.; Engelman, A.; Fuchs, J. R.; Kvaratskhelia, M. *J. Biol. Chem.* **2013**, *288*, 15813.
46. Desimmie, B. A.; Schrijvers, R.; Demeulemeester, J.; Borrenberghs, D.; Weydert, C.; Thys, W.; Vets, S.; Van Remoortel, B.; Hofkens, J.; De Rijck, J.; Hendrix, J.; Bannert, N.; Gijsbers, R.; Christ, F.; Debyser, Z. *Retrovirology* **2013**, *10*, 57.
47. Galan, A. A.; Chen, J.; Du, H.; Forsyth, T.; Huynh, T. P.; B., J. H. W.; Kearney, P.; Leahy, J. W.; Lee, M. S.; Mann, G.; Ridgway, B. H.; Takeuchi, C. S.; Zhou, P. WO 2008/042282 A2, 2008.
48. Maddry, J. A.; Ananthan, S.; Goldman, R. C.; Hobrath, J. V.; Kwong, C. D.; Maddox, C.; Rasmussen, L.; Reynolds, R. C.; Secrist, J. A., 3rd; Sosa, M. I.; White, E. L.; Zhang, W. *Tuberculosis (Edinb)* **2009**, *89*, 354.
49. Perchellet, E. M.; Perchellet, J. P.; Baures, P. W. *J. Med. Chem.* **2005**, *48*, 5955.
50. Al-Mawsawi, L. Q.; Fikkert, V.; Dayam, R.; Witvrouw, M.; Burke, T. R., Jr.; Borchers, C. H.; Neamati, N. *Proc. Natl. Acad. Sci. U.S.A.* **2006**, *103*, 10080.
51. Suite 2012: *LigPrep, v.*, Schrödinger, LLC.: New York, NY, 2012.
52. Jones, G.; Willett, P. *Curr. Opin. Biotechnol.* **1995**, *6*, 652.
53. Jones, G.; Willett, P.; Glen, R. C.; Leach, A. R.; Taylor, R. *J. Mol. Biol.* **1997**, *267*, 727.